Heliyon 10 (2024) e34875

Contents lists available at ScienceDirect

Heliyon

journal homepage: www.cell.com/heliyon

Research article

# Complexation of 3p-*C*-NETA with radiometal ions: A density functional theory study for targeted radioimmunotherapy

Danni Ramdhani [a,b,*], Hiroshi Watabe [b], Ari Hardianto [c], Regaputra S. Janitra [c]

[a] Department of Pharmaceutical Analysis and Medicinal Chemistry, Faculty of Pharmacy, Universitas Padjadjaran, Sumedang, Indonesia
[b] Division of Radiation Protection and Safety Control, Cyclotron and Radioisotope Center (CYRIC), Tohoku University, Sendai, Japan
[c] Department of Chemistry, Faculty of Mathematics and Natural Sciences, Universitas Padjadjaran, Sumedang, Indonesia

A B S T R A C T

Bifunctional chelators (BFCs) are vital in the design of effective radiopharmaceuticals, as they are able to bind to both a radiometal ion and a targeting vector. The 3p-*C*-NETA or 4-[2-(bis-carboxy-methylamino)-5-(4-nitrophenyl)-entyl])-7-carboxymethyl-[1,4,7]tri-azonan-1-yl acetic acid is a novel and promising BFC, developed for diagnostic and therapeutic purposes. The binding affinity between the BFC and radiometal ion significantly impacts their effectiveness. Predicting the equilibrium constants for the formation of 1:1 radiometals/chelator complexes (log $K_1$ values) is crucial for designing BFCs with improved affinity and selectivity for radiometals. The purpose of this study is to evaluate the complexation of $Ga^{3+}$, $Tb^{3+}$, $Bi^{3+}$, and $Ac^{3+}$ radiometal ions with 3p-*C*-NETA using density functional theory (B3LYP and M06-HF functional) and 6-311G(d)/SDD basis sets, where the 1,4,7,10-tetrazacyclodecane-1,4,7,10-tetracetic acid (DOTA) was employed as a benchmark. Formation of the $[Ac^{3+}$(3p-*C*-NETA)$(H_2O)]^-$ complexes is predicted to be markedly less stable compared to the other complexes, exhibiting the lowest chemical hardness and the highest chemical softness. Additionally, the chelation stability of the complexes is mainly determined by ligand-ion and ion-water interactions, which depend on the atomic charge and atomic radius of the metal ion.

## 1. Introduction

The application of radioisotopes in radiopharmaceuticals has been growing rapidly as a radiotracer for cancer imaging via positron emission tomography (PET) or single photon emission tomography (SPECT), and also for therapeutic purposes by utilizing β, α -particles, or auger electron emission [1,2]. Bifunctional chelates (BFCs) are an important component in the successful use of radiopharmaceutical compounds [3]. BFCs play a critical role in radiopharmaceutical design by binding radiometals strongly and forming complex radiometal compounds. These chelators, also known as ligands, are essential for attaching radiometals to targeting vectors such as peptides or antibodies. BFCs need to exhibit high thermodynamic stability and fast radiolabeling kinetics under mild conditions to effectively deliver the radiometals to their intended targets. Without BFCs, radiopharmaceutical compounds could not effectively and selectively deliver the radiometals for diagnostic or therapeutic purposes [4,5].

DOTA as an important chelator in a series of compounds approved by the FDA for the diagnosis ($^{68}$Ga-DOTA-TATE) and treatment ($^{177}$Lu-DOTA-TATE) of somatostatin receptor positive neuroendocrine tumors. DOTA has been widely used as a stable chelator of tripositive radiometals such as $^{68}Ga^{3+}$, $^{111}In^{3+}$, $^{177}Lu^{3+}$, $^{86/90}Y^{3+}$, $^{44/47}Sc^{3+}$.

Steric restrictions and electrostatic interactions are the main driving forces for radiometal-ligand bonding in complexes. The large ionic radius of the metal ion leads to the creation of kinetically labile complexes because the stability of electrostatic interactions scales as the ratio of charge over distance [6]. The ionic radius of the metal ion has an inverse relationship with the thermodynamic stability

* Corresponding author. Department of Pharmaceutical Analysis and Medicinal Chemistry, Faculty of Pharmacy, Universitas Padjadjaran, Sumedang, Indonesia.
*E-mail address:* d.ramdhani@unpad.ac.id (D. Ramdhani).

https://doi.org/10.1016/j.heliyon.2024.e34875
Received 18 December 2023; Received in revised form 13 July 2024; Accepted 17 July 2024
Available online 20 July 2024

of DOTA metal ion complexes; bigger central metal ions result in less stable complexes. A ligand that effectively binds and retains these radiometals is required for a therapeutic and diagnostic approach [7].

However, one major disadvantage of DOTA is the requirement for high temperatures during the radiolabeling process, which can be problematic for heat-sensitive vector molecules. This limitation has prompted the search for alternative chelators, such as 3p-*C*-NETA, that can provide similar or improved stability and kinetics without the need for high temperatures [8,9].

3p-*C*-NETA or 4-[2-(bis-carboxy-methylamino)-5-(4-nitrophenyl)-entyl])-7-carboxymethyl-[1,4,7]tri-azonan-1-yl acetic acid possesses a macrocyclic NODA (1,4,7-triazacyclononane-N,N′-diacetic acid) backbone (Fig. 1) and a flexible acyclic tridentate pendant arm. It is proposed to quickly start coordination with the radiometal. It is a promising chelator in terms of kinetics and stability for diagnostic purposes ($^{68}$Ga and $^{18}$F) and also for therapeutic purposes, such as β-emitters ($^{90}$Y and $^{177}$Lu), auger electrons ($^{161}$Tb), and α-emitters ($^{213}$Bi) [10–12].

In this study, we report for the first-time radiolabeling behavior of the 3p-*C*-NETA chelator using DOTA as a benchmark with DFT (density functional theory) calculations to compare the formation constant of the ligand-radiometal complex. We made a comparison of chelators (DOTA and 3p-*C*-NETA) to radiometals $Ga^{3+}$, $Tb^{3+}$, $Bi^{3+}$, and $Ac^{3+}$. DFT based *ab initio* simulations of formed complexes were used for investigation into the energy stability and structure-property relationships from a quantum mechanics perspective. The structures of the ligands (DOTA and 3p-*C*-BETA) are in Fig. 1, used in DFT calculations on complex formation with $Ga^{3+}$, $Tb^{3+}$, $Bi^{3+}$, and $Ac^{3+}$.

DFT calculations were applied to predict the stable structures and thermodynamic stability constants of the complexes. Vibration frequency computations were performed to ensure the absence imaginary frequencies [13]. Application of the implicit solvation model as an approach for typical conditions of radiosynthesis and application of radiopharmaceutical compounds based on the stability of radiometal-ligands by *in vitro* testing [14,15]. We used M06-HF/6-311G(d) and B3LYP/6-311G(d) as the functional/basis sets by applying solvation model density (SMD) and conductor-like screening model (COSMO).

## 2. Computational details

In this study, DFT calculations were performed using the Gaussian 16 program [16]. The new hybrid meta-exchange-correlation full-Hartree–Fock (M06-HF) and Becke, 3-parameter, Lee-Yang-Parr (B3LYP) were used as the density functionals. The 6-311G(d) basis set was used for DOTA and 3p-*C*-NETA, while GENECP basis set was applied for the radiometal ions for all complexes. The choice of these functionals and basis sets was based on their proven accuracy and reliability in predicting the thermodynamic properties of metal-ligand complexes. Additionally, implicit solvation models, such as COSMO and SMD, were applied to mimic typical conditions of radiosynthesis and the stability of radiometal-ligands *in vitro*. These models help account for the effects of solvation on the stability and properties of the complexes [17].

### 2.1. DFT calculations

In this work, we investigated the complexes formed between $Ga^{3+}$, $Tb^{3+}$, $Bi^{3+}$, and $Ac^{3+}$ metals with 3p-*C*-NETA using DOTA as a benchmark. All geometry optimizations and frequency calculations were performed in the gas phase. The frequency calculation results were used to compute the overall adjustment for enthalpy and entropy at T = 298.15 K as well as to verify the geometric structure with the lowest energy on the potential energy surface. To determine the gas phase free energy for each structure and the differences $\Delta G^{\circ}g$, these results will be combined with the total energy DFT.

We determined single-point aqueous solvation free energies, $\Delta G^{*}_{solv}$, using the gas-phase geometries and both the COSMO and the SMD model solvation to construct the thermodynamic cycle. Then from the cycle, we computed the stability constants, log $K_1$, and the free-energy changes in the aqueous phase, $\Delta G_{aq}$.

### 2.2. Conceptual DFT-based characteristic

The DFT-based structural characteristics (chemical hardness, η; and softness, S) were calculated using the following equations:

$$\eta = \frac{(IP - EA)}{2} \quad S = \frac{1}{2\eta} \tag{1}$$

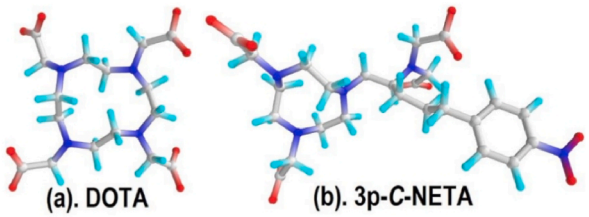


**Fig. 1.** (a). DOTA; coordination number = 8; (b) 3p-C-NETA; coordination number = 8.

where IP (ionization potential), and EA (electron affinity), were obtained from DFT calculations for the frontier orbital energies, HOMO (Highest Occupied Molecular Orbital) and LUMO (Lowest Unoccupied Molecular Orbital) [14,18].

## 3. Results and discussion

### 3.1. DFT calculation

A formation constant in coordination chemistry is an equilibrium constant describing the formation of a complex from its central ion and attached ligands in solution. It is also known as a stability constant or binding constant. In this study, we focused on the formation of a 1:1 complex by the binding of ligands (3p-*C*-NETA or DOTA) to the radiometals. The calculation of the formation constant $K_1$ from the 1:1 complex/ligand ratio at equilibrium conditions $M + L \rightleftharpoons ML$ is related to the change in the Gibbs energy of the reaction occurring in solution, $\Delta G_{aq}$. The strength of the metal-ligand interaction is quantified by individual log $K_1$ values, and the difference between the log $K_1$ values of two metal ions indicates the degree of selectivity [19,20].

$$M + L \rightleftharpoons ML \quad \log K_1 = \log \frac{[M][L]}{L} = \frac{-\Delta G_{aq}}{2.303RT} \tag{2}$$

The thermodynamic cycle in Fig. 2 serves as the reference for calculating $\Delta G_{aq}$.

The free-energy changes of the metal and ligand bindings in the gas phase are represented in this process by the symbol $\Delta G^{\circ}_{g}$, where $\Delta G^{*}_{solv}$ indicates the free energy needed to solvate 1 mol of solute from its gaseous state into an aqueous phase [21]. The equation calculates the value of $\Delta G^{\circ}_{g}$ for normal ideal gas conditions at 1 atm (24.46 mol/L) to 1 M (1 mol/L).

$$\Delta G^{o\,\rightarrow *} = -T\,\Delta S^{0\,\rightarrow *} = RT\ \mathrm{In}\ (Vo/V^{*}) = R.T.\mathrm{In}\ (24.46)$$

$$= 1.89\ \mathrm{kcal/mol}\ (T = 298.15\ K)$$

Calculation corrections are especially important when a pure solvent $H_2O_{(l)}$ is chosen as the reference state for the solvent, the state of the system is represented by $G_{aq}^{*} = G_{aq}^{*} + RT\ \ln([H_2O])$. The free-energy change required to move a solvent from a standard-state solution-phase concentration of 1 M to a standard-state pure liquid, 55.34 M, is calculated by $RT\ \ln([H_2O]) = 2.38$ kcal/mol [19,22].

We performed DFT calculations to calculate stability constants of complexes formed from metals ($Ga^{3+}$,$Tb^{3+}$, $Bi^{3+}$, and $Ac^{3+}$) with 3p-*C*-NETA ligands, respectively. Additionally, formation constants of the DOTA complex of each radiometals were calculated and used as a benchmark. Ligands will form complexes with metals with oxidation stability in $Ga^{3+}$, $Tb^{3+}$, $Bi^{3+}$, and $Ac^{3+}$respectively.

Targeted alpha treatment (TAT), which uses $^{225}Ac$ ($t_{1/2}$ = 9.9 d) to emit four α particles, is a potentially effective therapeutic approach that uses radionuclides that produce α particles to destroy tumour cells [23,24]. The DFT analyses of the $Ac^{3+}$ ion with 4–11 water molecules showed that $[Ac(H_2O)_9]^{3+}$ is the most stable in both gas phase and aqueous phase (COSMO model), which served as the inspiration for this choice of coordination number (CN) 9, and Ac with CN 9 has a large atomic radius of 1220 Å [25,26]. In addition, the daughter of $^{225}Ac^{3+}$, $^{213}Bi^{3+}$ ($t_{1/2}$ = 45.6 min), is easily obtained from $^{225}Ac/^{213}Bi$ generators and along its decay chain emits one α particle. Based on the characteristics of the donor atoms, the solvent, and the polydentate ligand, $Bi^{3+}$ exhibited a very variable coordination number (3–10) and a frequent irregular coordination geometry. Furthermore, even in highly acidic solutions, $Bi^{3+}$ hydrolyzes relatively quickly in aqueous solutions. As a result, the development of hydrolysis products makes studying $Bi^{3+}$ complexes in aqueous solutions difficult. Furthermore, other studies have proposed $Bi^{3+}$ forms 6 coordinates with pentagonal pyramidal geometry and directed stereochemically towards active 6s [2] lone pair and has the radius of ion at six coordination number is 1.03 Å [27–29].

Terbium in medical applications is very useful, because it has four isotopes that are used both for diagnostic purposes, such as $^{152}Tb$ ($\beta^{+}$ emitter, $t_{1/2}$ = 17.5 h) for positron emission tomography (PET), and $^{155}Tb$ (EC, γ-emitter, $t_{1/2}$ = 5.32 days) for single photon emission computed tomography (SPECT). Furthermore, terbium isotopes can also be used for therapeutic purposes, $^{149}Tb$ (α-emitter, $t_{1/2}$ = 4.12 h) and $^{161}Tb$ (β− emitter, $t_{1/2}$ = 6.90 days) on the other hand can be applied in targeted alpha (α) and beta (β) therapy, respectively. Single-crystal X-ray diffraction analysis of the terbium(III) complex in which the coordination number of the metal atom is nine, has the smaller effective ionic radius of 1.095 Å [30,31].

Gallium-68 is a widely used radioisotope for diagnostic imaging applications in positron emission tomography (PET). In order to create BFCs that enable more complex receptor targeting, coordination chemists must therefore create new chelate frameworks that can stable $Ga^{3+}$ (in a given coordination geometry). Thermodynamic studies have established the superior stability of six-coordinated of $Ga^{3+}$ complexes, with an ionic radius of 0.62 Å, reported by Hancock and Martell [32].

DFT was performed with Gaussian 16 to complete the calculations, and the ChemCraft software was used to visualize the structure graphically (Figs. S1–S4). The DFT calculations in this study employed M06-HF as a hybrid density functional due to its advantages in

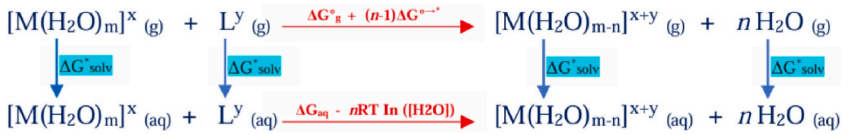


**Fig. 2.** Thermodynamic cycle used to calculate $\Delta G_{aq}$.

computing main group thermochemistry, thermochemical kinetics, noncovalent interactions, excited states, and transition elements [33]. In addition, M06-HF has good self-interaction error (SIE) in DFT as indicated by the small average mean unsigned errors (average MUE) (in kcal/mol), when compared to the functional PBE and B3LYP that are commonly used [34,35].

We performed DFT calculations by computing the formation constant of the ligands and complexes formed. Fig. 3 shows the representative equilibrium geometries of actinium ions with nine coordinated water molecules, $[Ac(H_2O)_9]^{3+}$, $[3p\text{-}C\text{-}NETA]^{4-}$, and their complex, $[Ac(3p\text{-}C\text{-}NETA)(H_2O)]^{-}$.

The classification of the atoms in the ligands-radiometal ion complex, from geometry optimization, was performed with the objective of making the interpretation of the data clearer. It was done by evaluating at the atoms' positions, connectivity, and various functional groups, which impact how their chemical environments differ from one another (Fig. 4).

We determined single-point aqueous solvation free energies, $\Delta G^*_{solv}$, using the geometries of the gas phase, and we used both the SMD model and the conductor-like screening model (COSMO) to evaluate the electrostatic interaction of a molecule with a solvent. The estimates for formation constants could be further enhanced by using computationally intensive techniques like explicit solvent quantum calculations [36]. The thermodynamic cycle can be completed to get the formation constants, log $K_1$, and the free-energy changes in the aqueous phase, $\Delta G_{aq}$, (see Supplementary Tables S1 and S2). The systematic errors within the computational methods may be largely cancelled using the deftly planned thermodynamic cycles [19].

DFT calculations for the formation constants (log $K_1$) of the radiometal-ligand complex in the gas phase, and the solvation models (SMD and COSMO) are reported in Table 1. The 3p-*C*-NETA ligand's formation constant computation reveals that $Ac^{3+}$ has a lower stability of complex formation than $Ga^{3+}$, $Tb^{3+}$, $Bi^{3+}$. This is in accordance with radiochemical conversion (RCC) that has been reported by Ahenkorah et al. radiolabeling studies with $Ac^{3+}$. The formation of the $^{225}Ac^{3+}$ complex with 3p-*C*-NETA at a concentration of 10 μM was carried out at a temperature variation of 25; 55; and 95 °C obtained an RCC below 90 % which does not meet the requirements. Increasing the temperature of the reaction is insufficient to accelerate the kinetics of the formation of the [$^{225}$Ac]Ac-3p-*C*-NETA complex [10]. In contrast, with the same labeling conditions, radiolabeling the radiometals $^{68}Ga^{3+}$, $^{161}Tb^{3+}$, and $^{213}Bi^{3+}$ with 3p-*C*-NETA showed significantly higher complexation yields, at 95 °C labeling conditions of 97.7 %, 97.9 %, and 98.6 %, respectively. The results indicate that the tridentate pendant acyclic donors in 3p-*C*-NETA are not effective enough to trap $Ac^{3+}$ which has a large atomic radius, in contrast to $Ga^{3+}$, $Tb^{3+}$, $Bi^{3+}$ which has a smaller atomic radius [11,24].

Furthermore, DFT calculations provide the formation constant of the radiometals-DOTA complex, where $Ac^{3+}$ also shows the lowest labeling efficiency compared to the formation of complexes with $Ga^{3+}$, $Tb^{3+}$, and $Bi^{3+}$. DOTA ($N_4O_4$) provides octadentate coordination via four tertiary amine nitrogen donors and four independent carboxylic acid arms, having insufficient cavities to trap $Ac^{3+}$ ions giving rise to the formation of kinetically labile complexes [24]. Some investigations that revealed losses of $^{225}$Ac-DOTA complex *in vitro* and *in vivo* have additionally raised into doubt the kinetics and stability of the $^{225}$Ac-DOTA complex [37].

In addition, analysis of interatomic distances between radiometal Ions ($Ga^{3+}$, $Tb^{3+}$, $Bi^{3+}$, and $Ac^{3+}$) with ligands 3p-*C*-NETA heteroatoms in the optimized structure, indicates oxygen and nitrogen atoms are weakest coordinated to $Ac^{3+}$ compared to other radiometals, with a mean distance the largest are Ac–O and Ac–N; 2584 and 2854 Å. This also holds true for the $Ac^{3+}$ and DOTA complexes, the mean interatomic distance of Ac–O and Ac–N gives the largest distances of 2576 and 2886 Å (Supplementary Tables S3 and S4). $Ac^{3+}$ with a large atomic radius forms a long interatomic distance with oxygen and nitrogen atoms, so that $Ac^{3+}$ is not strong enough to bind oxygen and nitrogen atoms, resulting in a low complex formation constant.

### 3.2. Conceptual DFT-based properties

Several chemical reactivity descriptors have been proposed as a result of research into various aspects of pharmacological sciences, such as drug design. DFT can calculate the concepts of potential importance of reactivity descriptors such as chemical potential, electronegativity, hardness, softness, and electrophilicity index as a starting point [38]. Ionization potential refers to an atom's or molecule's ability to donate electrons, whereas electron affinity refers to its ability to attract electrons. Chemical hardness, which is related to chemical system stability, indicates the resistance to changes in electron distribution. Global softness, which is related to the reactivity of the chemical system, is the inverse of hardness [14,39]. The reactivity index information: ionization potential (IP), electron affinity (EA), electrodonating power ($\omega^-$), electroaccepting power ($\omega^+$) and net electrophilicity ($\Delta\omega^{\pm}$) for ions radiometals,

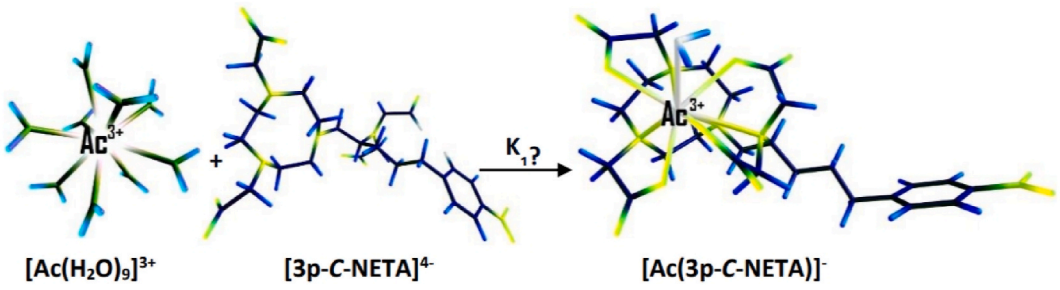


**Fig. 3.** Representative equilibrium geometries of the Actinium ion with the coordinated water molecules, $[Ac(H_2O)_9]^{3+}$, $[3p\text{-}C\text{-}NETA]^{4-}$), and their complex $[Ac(3p\text{-}C\text{-}NETA)(H_2O)]^{-}$

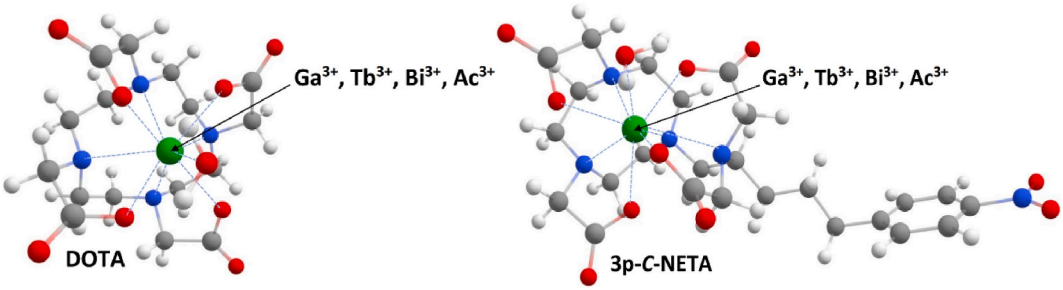


**Fig. 4.** Conformation of the 3p-*C*-NETA-radiometal ion complexes compared with DOTA complexes. Intermolecular distances between nearby heteroatoms and radiometal ions are illustrated in the figures by blue dashed-lines, where the geometric structure of 3p-*C*-NETA and DOTA is the result of geometry optimization. (For interpretation of the references to colour in this figure legend, the reader is referred to the Web version of this article.)

**Table 1**
Calculated formation constants (log $K_1$) for the complexes.

| Ligands | Metals | M06-HF/6-311G(d) | | | B3LYP/6-311G(d) | | |
|---|---|---|---|---|---|---|---|
| | | Log $K_1$ (Gas) | Log $K_1$ (SMD) | Log $K_1$ (COSMO) | Log $K_1$ (Gas) | Log $K_1$ (SMD) | Log $K_1$ (COSMO) |
| $[DOTA]^{4-}$ | $Ga^{3+}$ | 891.49 | 46.86 | 68.18 | 666.71 | 48.00 | 64.13 |
| | $Tb^{3+}$ | 828.33 | 37.59 | 49.66 | 604.10 | 39.63 | 56.73 |
| | $Bi^{3+}$ | 833.52 | 46.95 | 54.86 | 611.44 | 52.55 | 69.54 |
| | $Ac^{3+}$ | 815.83 | 22.75 | 28.17 | – | – | – |
| $[3p\text{-}C\text{-}NETA]^{4-}$ | $Ga^{3+}$ | 644.51 | 54.56 | 67.98 | 635.23 | 45.61 | 60.07 |
| | $Tb^{3+}$ | 566.10 | 32.18 | 39.88 | 557.99 | 29.29 | 37.91 |
| | $Bi^{3+}$ | 573.15 | 42.85 | 47.66 | 568.88 | 42.89 | 57.10 |
| | $Ac^{3+}$ | 556.17 | 22.55 | 27.71 | – | – | – |

ligands, and complexes are shown in Table 2.

The DFT calculation for free ions shows that for $Ac^{3+}$, compared to $Ga^{3+}$, $Tb^{3+}$, and Bi [3] has a larger ionic radius, hence, the observed lower chemical hardness, which is consistent with the findings that $Ac^{3+}$ has a larger atomic radius than $Ga^{3+}$, $Tb^{3+}$and $Bi^{3+}$. Furthermore, DFT-based properties show that 3p-*C*-NETA has a lower chemical hardness than DOTA. Pearson's hard-soft acid-base (HSAB) concept governs how metals interact with their ligands, with "hard" ions interacting most strongly with "hard" ligands and the opposite being true [40]. The chemical hardness of the complex can explain its stability, with the DOTA complex containing radiometal $Ga^{3+}$ having a higher value and being more stable than $Tb^{3+}$, $Bi^{3+}$ and $Ac^{3+}$. In addition, chemical hardness also explains that 3p-*C*-NETA ligand is more stable in forming complexes with $Ga^{3+}$, $Tb^{3+}$and $Bi^{3+}$compared to $Ac^{3+}$.

## 4. Conclusion

DFT using M06-HF and B3LYP functional and 6-311G(d)/SDD basis sets were utilized to investigate interactions that occur in the complexation process of 3p-*C*-NETA with radiometal ions $Ga^{3+}$, $Tb^{3+}$, $Bi^{3+}$, and $Ac^{3+}$. We also apply the implicit solvation models SMD (solvation model density) and COSMO (conductor-like screening model), which can be used to model the electrostatic interaction between the solute and solvent. by adding a thermodynamic cycle approach, used to calculate $\Delta G_{aq}$. We also use the cleverly designed thermodynamic cycles, the systematic errors within the computational protocols may be largely cancelled.

Our study reveals that the formation constant 3p-*C*-NETA-$Ac^{3+}$ shows the lowest value compared to other complexes (3p-*C*-NETA-$Ga^{3+}$, 3p-*C*-NETA-$Tb^{3+}$, and 3p-*C*-NETA-$Bi^{3+}$). In addition, the 3p-*C*-NETA ligand's greater stability in forming complexes with $Ga^{3+}$, $Tb^{3+}$, and $Bi^{3+}$ than with $Ac^{3+}$ can also be explained by its chemical hardness. Furthermore, DOTA as the gold standard ligand indicates that it is not suitable for use with radiometal $Ac^{3+}$ which has a large atomic radius. In general, ligand-ion and ion-water interactions are governed by the atomic charge and atomic radius of the metal ion, which are the main factors contributing to chelation stability. $Ac^{3+}$ has a larger atomic radius, resulting in the formation of a kinetically unstable complex.

## Funding statement

This research did not receive any specific grant from funding agencies in the public, commercial, or not-for-profit sectors.

## CRediT authorship contribution statement

**Danni Ramdhani:** Writing – review & editing, Writing – original draft, Visualization, Resources, Methodology, Formal analysis, Data curation, Conceptualization. **Hiroshi Watabe:** Writing – review & editing, Supervision. **Ari Hardianto:** Writing – review &

**Table 2**
Ionization potential (IP), electron affinity (EA), electrodonating power (ω−), electroaccepting power ($\omega^+$), and net electrophilicity ($\Delta\omega^{\pm}$) for radiometal ions ($Ga^{3+}$, $Tb^{3+}$, $Bi^{3+}$, and $Ac^{3+}$); the ligands (DOTA and 3p-*C*-NETA); and the complexes calculated at the M06-HF with SDD basis set for radiometal ion and 6-311G(d) basis set for another atom. $Ga^{3+}$ calculated at M06-HF/6-31G(d). The results of computations in the gas phase are shown in the numbers below, whereas the numbers above represent the results in water (SMD).

| System | Energy (eV) | | | | | |
|---|---|---|---|---|---|---|
| | IP | EA | η | $\omega^-$ | $\omega^+$ | $\Delta\omega^{\pm}$ |
| $Ga^{3+}$ | 44.858 | 9.944 | 17.457 | 37.387 | 9.986 | 9.959 |
| | 67.613 | 31.344 | 18.134 | 94.504 | 45.026 | 45.015 |
| $Tb^{3+}$ | 24.731 | 0.444 | 12.144 | 14.335 | 1.748 | 1.678 |
| | 49.406 | 21.238 | 14.084 | 63.716 | 28.393 | 28.378 |
| $Bi^{3+}$ | 23.197 | 14.065 | 4.566 | 47.898 | 29.267 | 29.246 |
| | 42.693 | 33.544 | 4.575 | 178.439 | 140.321 | 140.315 |
| $Ac^{3+}$ | 24.060 | 0.497 | 11.782 | 14.010 | 1.731 | 1.660 |
| | 48.496 | 18.722 | 14.887 | 56.603 | 22.994 | 22.977 |
| $DOTA^{4-}$ | 8.500 | −3.086 | 5.793 | 2.710 | 0.003 | −0.366 |
| | −1.654 | −12.343 | 5.345 | 1.751 | 8.749 | 8.178 |
| 3p-*C*-$NETA^{4-}$ | 7.981 | 0.099 | 3.941 | 4.584 | 0.544 | 0.325 |
| | −1.420 | −6.656 | 2.618 | 1.422 | 5.460 | 4.757 |
| $[Ga(DOTA)]^-$ | 9.630 | −2.176 | 5.903 | 3.778 | 0.051 | −0.214 |
| | 7.352 | −4.104 | 5.728 | 1.758 | 0.134 | −0.435 |
| $[Ga(3p\text{-}C\text{-}NETA)]^-$ | 9.327 | 0.091 | 4.618 | 5.333 | 0.624 | 0.436 |
| | 7.152 | −1.429 | 4.291 | 2.921 | 0.060 | −0.283 |
| $[Tb(DOTA)(H_2O)]^-$ | 10.413 | −1.443 | 5.928 | 4.681 | 0.195 | −0.018 |
| | 8.022 | −4.024 | 6.023 | 2.084 | 0.085 | −0.395 |
| $[Tb(3p\text{-}C\text{-}NETA)(H_2O)]^-$ | 10.105 | 0.089 | 5.008 | 5.768 | 0.671 | 0.498 |
| | 8.031 | −1.430 | 4.731 | 3.393 | 0.092 | −0.202 |
| $[Bi(DOTA)(H_2O)]^-$ | 7.012 | −2.551 | 4.781 | 2.233 | 0.003 | −0.445 |
| | 4.240 | −4.177 | 4.209 | 0.542 | 0.510 | −1.334 |
| $[Bi(3p\text{-}C\text{-}NETA)(H_2O)]^-$ | 7.304 | 0.090 | 3.607 | 4.194 | 0.497 | 0.259 |
| | 4.863 | −1.524 | 3.193 | 1.670 | 0.001 | −0.598 |
| $[Ac(DOTA)(H_2O)]^-$ | 10.181 | 0.080 | 5.051 | 5.802 | 0.672 | 0.499 |
| | 8.038 | −1.011 | 4.524 | 3.686 | 0.173 | −0.098 |
| $[Ac(3p\text{-}C\text{-}NETA)(H_2O)]^-$ | 9.816 | 0.091 | 4.863 | 5.608 | 0.654 | 0.476 |
| | 8.040 | −1.443 | 4.742 | 3.389 | 0.091 | −0.204 |

editing, Supervision. **Regaputra S. Janitra:** Writing – review & editing, Validation, Supervision, Investigation, Formal analysis.

## Declaration of competing interest

The authors declare that they have no known competing financial interests or personal relationships that could have appeared to influence the work reported in this paper.

## Acknowledgements

I would like to thank Indonesia Endowment Fund for Education (LPDP) from the Ministry of Finance Republic Indonesia for granting the scholarship and supporting this research.

## Appendix A. Supplementary data

Supplementary data to this article can be found online at https://doi.org/10.1016/j.heliyon.2024.e34875.

## References

[1] W. Price, E. Orvig, C. Matching, Chelators to radiometals for radiopharmaceuticals, Chem. Soc. Rev. 43 (1) (2014) 260–290.
[2] L. Pimlott, S, A. Sutherland, Molecular tracers for the PET and SPECT imaging of disease, Chem. Soc. Rev. 40 (1) (2011) 149–162.
[3] T.I. Kostelnik, C. Orvig, Radioactive main group and rare earth metals for imaging and therapy, Chem. Rev. 119 (2) (2019) 902–956.
[4] K. Vermeulen, M. Vandamme, G. Bormans, F. Cleeren, Design and challenges of radiopharmaceuticals, Semin. Nucl. Med. 49 (5) (2019) 339–356.
[5] C. Barca, C.M. Griessinger, A. Faust, D. Depke, M. Essler, A.D. Windhorst, N. Devoogdt, K.M. Brindle, M. Schäfers, B. Zinnhardt, A.H. Jacobs, Expanding theranostic radiopharmaceuticals for tumor diagnosis and therapy, Pharmaceuticals 15 (1) (2022) 13.
[6] A.T. Nikki, J.W. Justin, Actinium-225 for targeted α therapy: coordination chemistry and current chelation approaches, Cancer Biother. Rad. 33 (8) (2018) 336–348.
[7] A. Hu, E. Aluicio-Sarduy, V. Brown, S.N. MacMillan, K.V. Becker, T.E. Barnhart, V. Radchenko, C.F. Ramogida, J.W. Engle, J.J. Wilson, Py-macrodipa: a janus chelator capable of binding medicinally relevant rare-earth radiometals of disparate sizes, J. Am. Chem. Soc. 143 (27) (2021) 10429–10440.

[8] J.M. Kelly, A. Amor-Coarasa, A. Nikolopoulou, D. Kim, C. Williams, S. Vallabhajosula, J.W. Babich, Assessment of PSMA targeting ligands bearing novel chelates with application to theranostics: stability and complexation kinetics of $^{68}Ga^{3+}$, $^{111}In^{3+}$, $^{177}Lu^{3+}$ and $^{225}Ac^{3+}$, Nucl. Med. Biol. 55 (2017) 38–46.

[9] S. Ballal, M.P. Yadav, C. Bal, R.K. Sahoo, M. Tripathi, Broadening horizons with $^{225}$Ac-DOTATATE targeted alpha therapy for gastroenteropancreatic neuroendocrine tumour patients stable or refractory to $^{177}$Lu-dotatate PRRT: first clinical experience on the efficacy and safety, Eur. J. Nucl. Med. Mol. Imag. 47 (4) (2020) 934–946.

[10] S. Ahenkorah, E. Murce, C. Cawthorne, J.P. Ketchemen, C.M. Deroose, T. Cardinaels, Y. Seimbille, H. Fonge, W. Gsell, G. Bormans, M. Ooms, F. Cleeren, 3p-C-NETA: a versatile and effective chelator for development of Al$^{18}$F-labeled and therapeutic radiopharmaceuticals, Theranostics 12 (13) (2022) 5971–5985.

[11] C.S. Kang, X. Sun, F. Jia, H.A. Song, Y. Chen, M. Lewis, H.-S. Chong, Synthesis and preclinical evaluation of bifunctional ligands for improved chelation chemistry of $^{90}$Y and $^{177}$Lu for targeted radioimmunotherapy, Bioconjugate Chem. 23 (9) (2012) 1775–1782.

[12] H.-S. Chong, X. Sun, Y. Chen, I. Sin, C.S. Kang, M.R. Lewis, D. Liu, V.C. Ruthengael, Y. Zhong, N. Wu, H.A. Song, Synthesis and comparative biological evaluation of bifunctional ligands for radiotherapy applications of $^{90}$Y and $^{177}$Lu, Bioorg. Med. Chem. 23 (5) (2015) 1169–1178.

[13] J. Foresman, A. Frisch, Exploring Chemistry with Electronic Structure Methods, third ed., 2015.

[14] F.Y. Adeowo, B. Honarparvar, A.A. Skelton, Density functional theory study on the complexation of NOTA as a bifunctional chelator with radiometal ions, J. Phys. Chem. A 121 (32) (2017) 6054–6062.

[15] B.A. Sorenson, S.S. Hong, H.C. Herbol, P. Clancy, How well do implicit solvation models represent intermolecular binding energies in organic-inorganic solutions? Comput. Mater. Sci. 170 (2019) 109138.

[16] M.J. Frisch, G.W. Trucks, H.B. Schlegel, G.E. Scuseria, M.A. Robb, J.R. Cheeseman, G. Scalmani, V. Barone, G.A. Petersson, H. Nakatsuji, X. Li, M. Caricato, A. V. Marenich, J. Bloino, B.G. Janesko, R. Gomperts, B. Mennucci, H.P. Hratchian, J.V. Ortiz, A.F. Izmaylov, J.L. Sonnenberg, Williams, F. Ding, F. Lipparini, F. Egidi, J. Goings, B. Peng, A. Petrone, T. Henderson, D. Ranasinghe, V.G. Zakrzewski, J. Gao, N. Rega, G. Zheng, W. Liang, M. Hada, M. Ehara, K. Toyota, R. Fukuda, J. Hasegawa, M. Ishida, T. Nakajima, Y. Honda, O. Kitao, H. Nakai, T. Vreven, K. Throssell, J.A. Montgomery Jr, J.E. Peralta, F. Ogliaro, M. J. Bearpark, J.J. Heyd, E.N. Brothers, K.N. Kudin, V.N. Staroverov, T.A. Keith, R. Kobayashi, J. Normand, K. Raghavachari, A.P. Rendell, J.C. Burant, S. S. Iyengar, J. Tomasi, M. Cossi, J.M. Millam, M. Klene, C. Adamo, R. Cammi, J.W. Ochterski, R.L. Martin, K. Morokuma, O. Farkas, J.B. Foresman, D.J. Fox, Gaussian 16 Rev. D.01, 2016.

[17] M. Bursch, J.-M. Mewes, A. Hansen, S. Grimme, Best-practice DFT protocols for basic molecular computational chemistry, Angew. Chem. Int. Ed. 61 (42) (2022) e202205735.

[18] S. Saha, M.K. Mishra, C.M. Reddy, G.R. Desiraju, From molecules to interactions to crystal engineering: mechanical properties of organic solids, Acc. Chem. Res. 51 (11) (2018) 2957–2967.

[19] H. Chen, R. Shi, H. Ow, Predicting stability constants for terbium(III) complexes with dipicolinic acid and 4-substituted dipicolinic acid analogues using density functional theory, ACS Omega 4 (24) (2019) 20665–20671.

[20] A. Mitrofanov, N. Andreadi, V. Korolev, S. Kalmykov, A search for a DFT functional for actinide compounds, J. Chem. Phys. 155 (16) (2021) 161103.

[21] J.P. Holland, Predicting the thermodynamic stability of zirconium radiotracers, Inorg. Chem. 59 (3) (2020) 2070–2082.

[22] S.A. Cotton, P.R. Raithby, A. Shield, J.M. Harrowfield, A comparison of the structural chemistry of scandium, yttrium, lanthanum and lutetium: a contribution to the group 3 debate, Coord. Chem. Rev. 455 (2022) 214366.

[23] M.R. McDevitt, D. Ma, J. Simon, R.K. Frank, D.A. Scheinberg, Design and synthesis of $^{225}$Ac radioimmunopharmaceuticals, Appl. Radiat. Isot. 57 (6) (2002) 841–847.

[24] N.A. Thiele, J.J. Wilson, Actinium-225 for targeted α therapy: coordination chemistry and current chelation approaches, Cancer Biother. Radiopharm. 33 (8) (2018) 336–348.

[25] Y. Gao, P. Grover, G. Schreckenbach, Stabilization of hydrated AcIII cation: the role of superatom states in actinium-water bonding, Chem. Sci. 12 (7) (2021) 2655–2666.

[26] G.J.-P. Deblonde, M. Zavarin, A.B. Kersting, The coordination properties and ionic radius of actinium: a 120-year-old enigma, Coord. Chem. Rev. 446 (2021) 214130.

[27] R. Eychenne, M. Chérel, F. Haddad, F. Guérard, J.-F. Gestin, Overview of the most promising radionuclides for targeted alpha therapy: the “hopeful eight.”, Pharmaceutics 13 (6) (2021) 906.

[28] A. Hu, V. Brown, S.N. MacMillan, V. Radchenko, H. Yang, L. Wharton, C.F. Ramogida, J.J. Wilson, Chelating the alpha therapy radionuclides $^{225}Ac^{3+}$ and $^{213}Bi^{3+}$ with 18-membered macrocyclic ligands macrodipa and py-macrodipa, Inorg. Chem. 61 (2) (2022) 801–806.

[29] D.J. Fiszbein, V. Brown, N.A. Thiele, J.J. Woods, L. Wharton, S.N. MacMillan, V. Radchenko, C.F. Ramogida, J.J. Wilson, Tuning the kinetic inertness of $Bi^{3+}$ complexes: the impact of donor atoms on diaza-18-crown-6 ligands as chelators for $^{213}$Bi targeted alpha therapy, Inorg. Chem. 60 (12) (2021) 9199–9211.

[30] I. Cassells, S. Ahenkorah, A.R. Burgoyne, M. Van de Voorde, C.M. Deroose, T. Cardinaels, G. Bormans, M. Ooms, F. Cleeren, Radiolabeling of human serum albumin with terbium-161 using mild conditions and evaluation of in vivo stability, Front. Med. 8 (2021) 675122.

[31] T. Gregório, S.O.K. Giese, G.G. Nunes, J.F. Soares, D.L. Hughes, Crystal structures of two mononuclear complexes of terbium(III) nitrate with the tripodal alcohol 1,1,1-tris(Hydroxymethyl)Propane, Acta Crystallogr E Crystallogr Commun 73 (Pt 2) (2017) 278–285.

[32] G. Bandoli, A. Dolmella, F. Tisato, M. Porchia, F. Refosco, Mononuclear six-coordinated Ga(III) complexes: a comprehensive survey, Coord. Chem. Rev. 253 (1) (2009) 56–77.

[33] Y. Zhao, D.G. Truhlar, The M06 suite of density functionals for main group thermochemistry, thermochemical kinetics, noncovalent interactions, excited states, and transition elements: two new functionals and systematic testing of four M06-class functionals and 12 other functionals, Theor. Chem. Acc. 120 (1) (2008) 215–241.

[34] J.L. Bao, L. Gagliardi, D.G. Truhlar, Self-interaction error in density functional theory: an appraisal, J. Phys. Chem. Lett. 9 (9) (2018) 2353–2358.

[35] H. Kruse, L. Goerigk, S. Grimme, Why the standard B3LYP/6-31g* model chemistry should not Be used in DFT calculations of molecular thermochemistry: understanding and correcting the problem, J. Org. Chem. 77 (23) (2012) 10824–10834.

[36] U. Ryde, P. Söderhjelm, Ligand-binding affinity estimates supported by quantum-mechanical methods, Chem. Rev. 116 (9) (2016) 5520–5566.

[37] K.A. Deal, I.A. Davis, S. Mirzadeh, S.J. Kennel, M.W. Brechbiel, Improved in vivo stability of actinium-225 macrocyclic complexes, J. Med. Chem. 42 (15) (1999) 2988–2992.

[38] P. Geerlings, F. De Proft, W. Langenaeker, Conceptual density functional theory, Chem. Rev. 103 (5) (2003) 1793–1874.

[39] R. Pal, P.K. Chattaraj, Chemical reactivity from a conceptual density functional theory perspective, J. Indian Chem. Soc. 98 (1) (2021) 100008.

[40] J.L. Reed, Hard and soft acids and bases: atoms and atomic ions, Inorg. Chem. 47 (13) (2008) 5591–5600.